

**Utilizing Pushover Analysis for
Seismic Performance of Steel Bridge Structures**

Thomas A. Ballard, P.E., Director of Structural Engineering
tom@scsolutions.com

Alex Krimotat, Vice President
alex@scsolutions.com

Robyn Mutobe, P.E., Senior Engineer
robyn@scsolutions.com

SC Solutions, Inc.
3211 Scott Blvd.
Santa Clara, CA 95050
Phone: (408) 486-6060
Fax: (408) 486-6083

ABSTRACT

Seismic retrofit of steel bridges requires more advanced analysis techniques to determine capacities and predict inelastic performance parameters. Normal engineering analysis practice assumes linear-elastic behavior for structural members, which fails to reliably account for re-distribution of forces due to member non-linear behavior and dissipation of energy due to material yielding. The performance criteria for the 1958 Carquinez Strait Bridges is “no-collapse” which implies that structural members may yield, exhibiting both material and geometric non-linear behavior, provided that sufficient reserve strength and ductility remains to prevent the structure from collapsing. With increasing construction costs and tighter budgets, a key component in removing over-conservatism in the final retrofit design and effecting a cost-efficient, yet sound design solution, is to take a more rigorous approach to the structural analysis. Advances in technology for computer hardware and software permitted the 1958 Carquinez Strait Bridge seismic retrofit project team to perform a non-linear dynamic analysis for the main span structure in order to better characterize the behavior of the bridge and quantify the damage the structure might sustain during a large seismic event. This paper discusses the non-linear pushover analysis, which was a key component of the non-linear dynamic analysis and of the overall retrofit design effort for the bridge. The development of the material properties for the steel members is discussed and results of the as-built, prototype retrofit and final retrofit pushover analyses for one of the bridge towers is used to examine the procedures and rationale implemented to perform a performance based analysis and design.

INTRODUCTION

The State of California designed the Carquinez Bridge east main structure and construction was completed in 1958. The project site is located between Solano and Contra Costa Counties, between the cities of Vallejo and Crockett, California. The 1958 Carquinez Bridge currently carries eastbound traffic on Interstate 80 from the greater San Francisco Bay Area to the Sacramento Valley. This 1022-meter long bridge spans the Carquinez Strait, a major shipping channel for the Sacramento River. Both the shipping channel and the vehicular artery that the Carquinez Bridge provides are considered important routes of commerce for the State of California.

The bridge has five spans consisting of two 153-meter anchor spans, one 46-meter center tower span, and two 336-meter interior spans. Each interior span is comprised of two 102-meter cantilever spans simply supporting a 132-meter long suspended span.

All analysis in support of the retrofit design was performed using the finite element program, ADINA (1). ADINA was specified by the State of California for the California Toll Bridge Seismic Retrofit Program because it permits the user to evaluate important non-linear behaviors for the bridge structures, such as, expansion joints, damping devices, bearings, contact and non-linear axial force-bending moment interaction.

This paper presents the results of the Tower 3 pushover analysis. A discussion of the development of moment-curvature properties for the non-linear members is presented. The procedures used to perform the collapse analysis and determine the behavior of individual members is also discussed. Results of the collapse analyses for the as-built, prototype retrofit and final retrofit designs are presented and discussed.

The purpose of the dynamic non-linear analysis effort (2) was to determine the structural response for the bridge steel members due to the postulated safety evaluation earthquake. As part of this effort, the capacities of the as-built and retrofit towers were determined via tower collapse, or “pushover,” analyses. These analyses investigated the mechanisms that could lead to collapse of the towers, including local and global buckling of members, axial tension failure, and plastic hinge formation due to moment yield or rupture. The collapse analyses were also used to determine the overall ductility of the tower structures and ductility of individual structural elements. Several prototype retrofit designs for the towers were evaluated and compared to the as-built tower capacities to determine the improvements in ductility realized through various retrofit configurations.

Prototype retrofit towers with all of the structural elements characterized as non-linear were later included in a full bridge model, shown in Figure 1, where the superstructure was modeled as elastic. The design earthquake motion was applied to the system, and the system was analyzed. Finally, superstructure members considered essential to the primary load-path, as well as members with significantly high demand-capacity ratios, were characterized using non-linear properties for subsequent earthquake analyses.

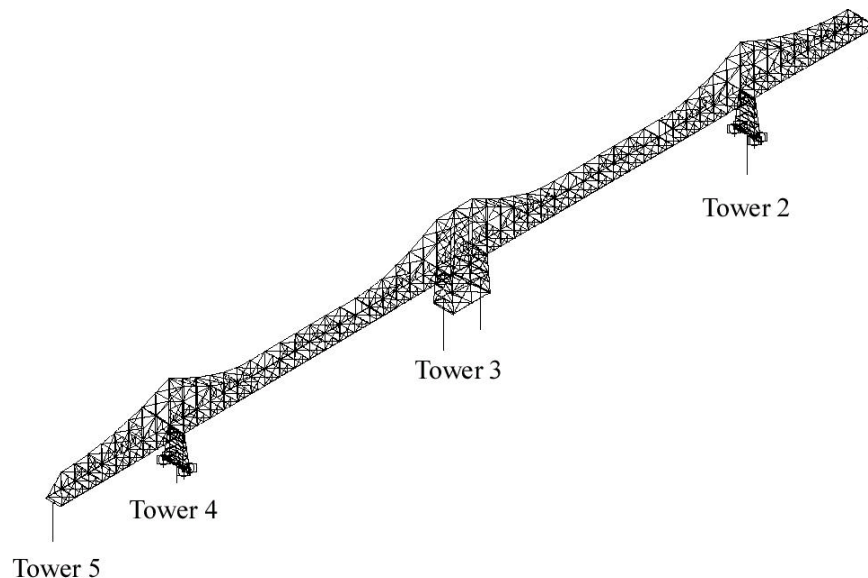


Figure 1 – 1958 Carquinez Bridge - Global ADINA Finite Element Model

MOMENT-CURVATURE BEAM ELEMENT

One of the latest features implemented in the ADINA program is a non-linear beam defined through moment-curvature and axial force-strain interaction. The development of this class of elements is an important advancement in the available tools for estimating the structural behavior in large bridge structures because of the size of such bridge models and the efficiency of these elements. For the non-linear analysis activity, most of the bridge truss and tower members that exhibited inelastic behavior were defined using non-linear moment-curvature ADINA beam elements.

The inelastic members were characterized using four sets of non-linear curves. These curves defined axial force-strain, bending moment-curvature for both bending axes, and torsion-twist. The axial force was coupled separately to each of the two bending moments and torsion, resulting in a family of curves for each principal direction. These families of curves thus defined the axial force-moment interaction for each element. In ADINA, axial force-strain curves must be symmetric for tension and compression. However, a different set of moment-curvature relationships may be defined for axial tension versus axial compression. In other words, moment-curvature curves need not be symmetric with respect to the sign of the axial force.

NON-LINEAR MEMBER PROPERTIES

Perhaps one of the most important issues for the analysis of the 1958 Carquinez Bridge was the establishment of reliable member properties, that is, moment-curvature and axial force-strain properties that properly represented the behavior of such members. Much effort was invested establishing these member properties (3).

Derivations of the axial force-strain and moment-curvature curves are based on established engineering mechanics principles that assume that strains can be linearly interpolated over the cross-section and curvatures, when combined with uniform axial strains, result in a non-linear stress distribution that can be integrated to determine resisting force and moment. Therefore, moment-curvature yield points and ultimate curvatures can be determined for any state of axial force-strain using the member's material yield stress and ultimate strains.

Moment-curvature and axial force-strain curves were simplified to bilinear curves in a manner that maintains the total energy of the theoretical curves, i.e., the total area under the theoretical curves and the simplified curves were equal. The moment-curvature curves contain, as a minimum, a yield point and a rupture, or ultimate curvature, point. Each moment-curvature curve corresponds to a specific member axial force. The range of axial forces in combination with the family of moment-curvature curves defines the interaction surface for the element. Figure 2 shows a typical set of these moment-curvature curves. The axial force curves were developed using weighted average section properties for the bridge's perforated members.

Above the critical local buckling compressive load, the bending resistance is considered to be zero. For both axial tension and flexure, the bending curvature rupture points correspond to either the ultimate tensile strength of the material, or the point at which bending will cause local buckling in one of the extreme fibers.

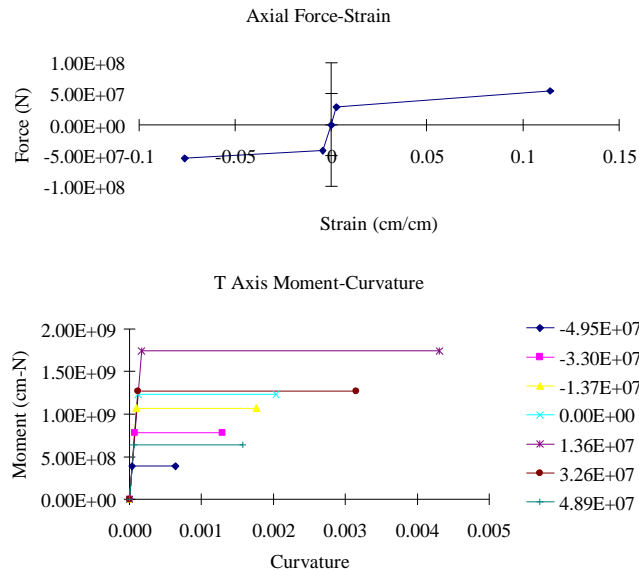


Figure 2 - Typical Member Properties

PUSHOVER ANALYSIS METHODOLOGY

For the pushover analyses, the geometry of the towers was extracted from the global ADINA model and each element in the tower structures was modified to capture its expected non-linear behavior. Before any non-linear analysis was implemented, rigorous tests including material properties, beam moment-curvature elements, and non-linear buckling behavior were conducted.

Implementation of Non-linear Elements

Each structural member with a high slenderness ratio was subdivided into four finite elements each defined using five integration points along their lengths. Components comprising individual members of x-brace systems, with probable out-of-plane collapse modes, were subdivided into two non-linear finite elements of equal length. For members with low slenderness ratios where collapse was considered improbable, no element subdivision was implemented.

Each element was offset from the work point of the connection. The length of the offset was taken from the work point as defined in the elastic model, to the last line of bolts in the gusset plate connecting the member to the joint. This offset of the end of each member from the connection work point was represented using rigid links. This implementation of rigid links implies that the retrofit design details would ensure that connection capacities exceeded member capacities by a minimum of 30 percent, thereby forcing any yielding to occur in the member rather than within the region of the connection. Where connections controlled, such as, for several members in the as-built structure, axial tension-strain curves were defined such that the tension rupture point corresponded to the capacity of the connection.

Tower Collapse Analysis

A key step in the evaluation of the behavior of the 1958 Carquinez Bridge structure was the individual tower collapse, or “push-over,” analyses. These analyses provided valuable insight to the structural characteristics of the as-built towers, as well as the effects of various retrofit alternatives on their displacement capacities.

Tower collapse analysis models for the as-built and prototype retrofit configurations were extracted from the elastic ADINA global model. Boundary conditions at the bases of the towers were defined consistent with the details of their support upon their respective caissons or pile caps. Where retrofit details permit the column legs freedom to uplift, contact surfaces were placed at the bottom of the legs with elastomeric bearing

pads modeled using linear or non-linear spring elements. Shear keys and restrainer beams were modeled per the design details, with end moment and axial force releases properly represented.

The top of each tower was constrained to a “push” node located at the tower plan center with the constraints defined consistent with details of force transfer between the bridge tower and superstructure. The constraint details included fixity of the top of each tower leg to the bridge, and shear transfer at the apex of top chevron bracing members and shear keys.

The dead weight of the tower structure was applied as the first step. The mass of the portion of the bridge superstructure that was supported by the tower was also applied as a vertical load to the push node in this step. Next, a displacement or rotation was applied to the push node in the direction of study and the displacement was increased until P- δ collapse of the tower occurred. Typically, the tower was “pushed” to collapse in the longitudinal and transverse directions, as well as in three intermediate directions at 30, 60, and 75 degree angles to the centerline of the bridge. A global twist (or rotation) was also applied to the “push” node in order to determine the torsional ductility of the tower. “Collapse” was defined to occur, and the solution was typically terminated, when the reaction at the push node peaked then dropped to less than 80% of the maximum value.

Several steps were required for post-processing results of tower collapse analyses. For all non-linear members, axial force, bending moments, curvatures, and member distortions, as well as total and plastic axial strains were evaluated.

A tower collapse scenario was constructed and displayed for the active frame in each push direction. The active frame is defined as the frame that is in the plane of the push load and thus active in resisting this load. A load-deflection curve was plotted for each tower collapse analysis, and important events along the collapse history were noted. For each significant event, a “snapshot” of the displaced shape of the structure is developed, and yield and/or rupture states of the elements in the frame are indicated along with the displacement associated with each members non-linear activity. The collapse scenario, in conjunction with the strain and distortion time histories, provided a good physical understanding of the behavior of the structure on both a component level and a global structural level. The collapse scenario showed clearly the yielding sequence and re-distribution of forces, which occurred when various elements yielded, ruptured in tension, or buckled in compression.

The collapse analyses were also useful for establishing displacement capacity envelopes for each tower structure. By applying push loads at various angles to the centerline of the bridge towers, the maximum displacements for each loaded direction were plotted on a polar graph, thereby defining the displacement capacity envelope. This envelope was useful when compared to maximum displacements of the towers from the global time history analyses.

AS-BUILT TOWER COLLAPSE ANALYSES

The ADINA non-linear finite element model for Tower 3 are shown in Figure 3. This figure indicates the final retrofit details and therefore corresponds to the final retrofit push model.

Tower 3 is the longitudinal anchor tower for the bridge seismic loads, therefore, the longitudinal frames were designed to resist significant load. The longitudinal load-resisting frames for Tower 3 are two sets of chevron-braced frames in the east and west elevations. Tower 3 stands approximately 41.5 meters (136 feet) high, and its width is 45.8 meters (150 feet).

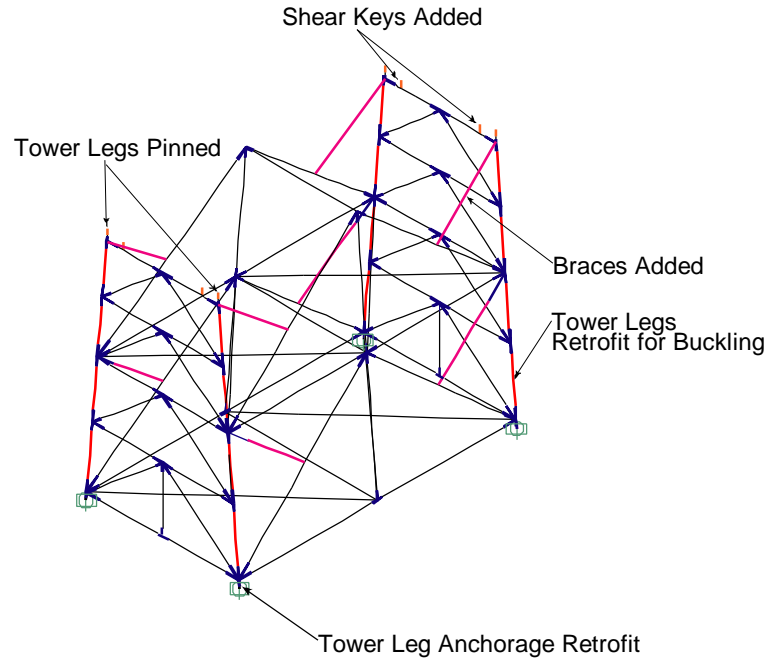


Figure 3 - Tower 3 ADINA Finite Element Model

Longitudinal Pushover - As-Built Tower 3

The Tower 3 longitudinal collapse load-deflection curve and collapse scenario plots are depicted in Figures 4 and 5, respectively. The tower remained elastic to a deflection of approximately 8.4 centimeters, at which time the lower compression chevron brace yielded. At a deflection of 10.4 centimeters, defined as Event Point A, several members reached their yield limits. The upper compression chevron yielded, the lower tension chevron yielded, and the lower compression chevron formed a hinge at the upper joint. The base of the compression leg also formed a hinge due to moment yield. The softening of the tower is evident from the load-deflection diagram, which clearly demonstrates a marked change in stiffness of the longitudinal resisting frame.

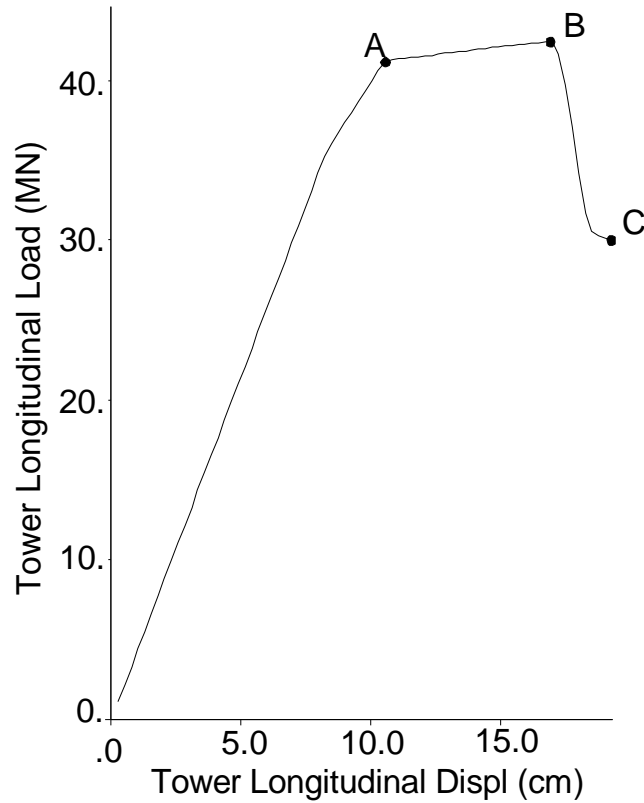


Figure 4 – As-Built Tower 3 – Load-Deflection Curve

The frame continued to exhibit a slight strain hardening until Event Point B was reached at a maximum tower load capacity of 42.3 MN and deflection of 16.5 centimeters. At Event Point B, the lower compression chevron formed hinges at the lower joint and middle. At this point, the frame rapidly lost its load capacity, and the lower compression chevron buckled because of the hinges that had formed along its length. At Event Point C, the deflection of the frame was 19.1 centimeters, and moment rupture of the middle hinge in the lower compression chevron occurred.

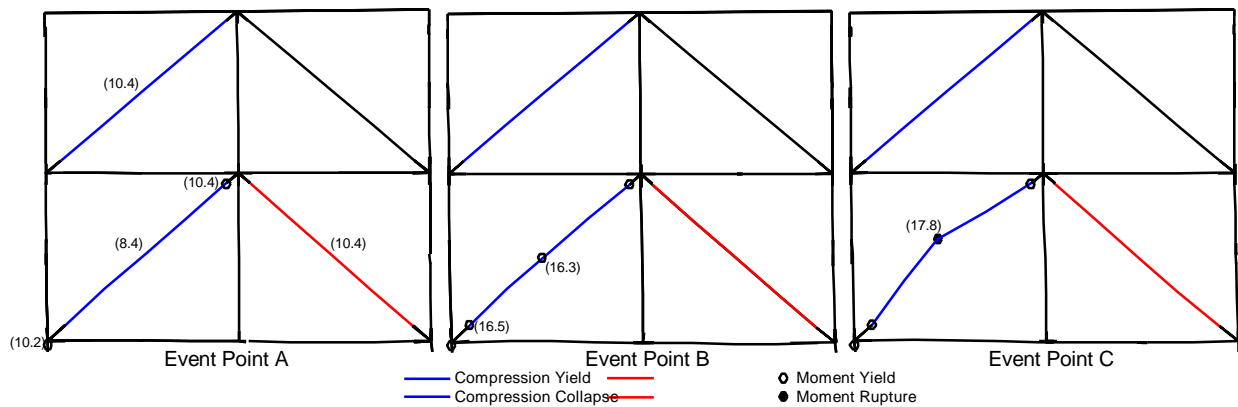


Figure 5 – As-Built Tower – Collapse Scenario

The tower displacement at Event Point B on the load-deflection curve was defined as the displacement ductility limit in the longitudinal direction.

BRIDGE TOWER RETROFIT COLLAPSE ANALYSES

After identifying deficiencies in displacement capacity as well as vulnerability of key members to net section fracture and early local buckling, retrofit measures for the tower were investigated via subsequent pushover analyses.

After performing the prototype retrofit pushover analyses for the tower, the design team made additional iterations on the retrofit designs for both towers to increase their longitudinal displacement capacities. Additionally, because the overall design philosophy required Tower 3 to be the longitudinal anchor for the bridge, the team sought to improve the lateral displacement ductility of the frame from the prototype retrofit to the final retrofit design.

The prototype Tower 3 retrofit consisted primarily of strengthening the connections and stiffening local elements to prevent local buckling. The final retrofit added additional bracing members to the chevrons in the longitudinal load-resisting frame of the tower to prevent early buckling. The final retrofit also added tie downs to the tower legs.

Longitudinal Pushover - Prototype Retrofit Tower 3

The prototype retrofit Tower 3 longitudinal collapse load-deflection curve is shown in Figure 6, and the collapse scenario is shown in Figure 7. At approximately 10.2 centimeters of deflection, yielding occurred in both compression chevron braces and the lower tension chevron. An appreciable decrease in stiffness was detected at a deflection of approximately 25.4 centimeters, Event Point A. This occurred after the upper tension chevron yielded, and several hinges had formed in the lower joints of the frame.

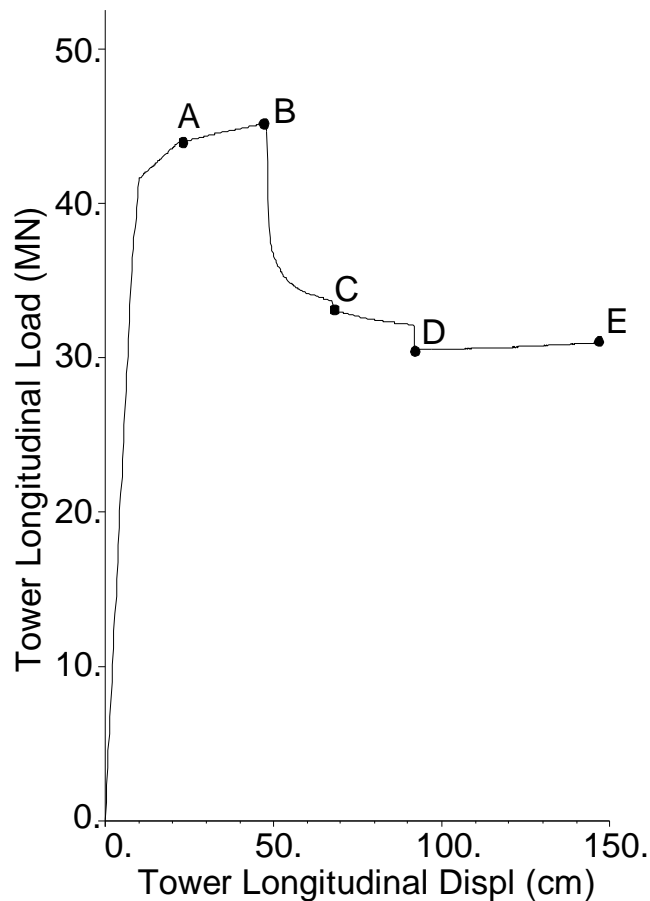


Figure 6 - Prototype Retrofit Tower 3- Load-Deflection Curve

Unlike the as-built configuration of the longitudinal frame of this tower, the prototype retrofit frame showed significantly higher displacement ductility between first yield and the first drop in load capacity. Event Point B occurred at approximately 49.3 centimeters and 44.7 MN of load, which is the maximum load capacity of the prototype retrofit frame. Hinging occurred most notably along the length of the lower compression chevron and at both joints of the mid-height horizontal beams.

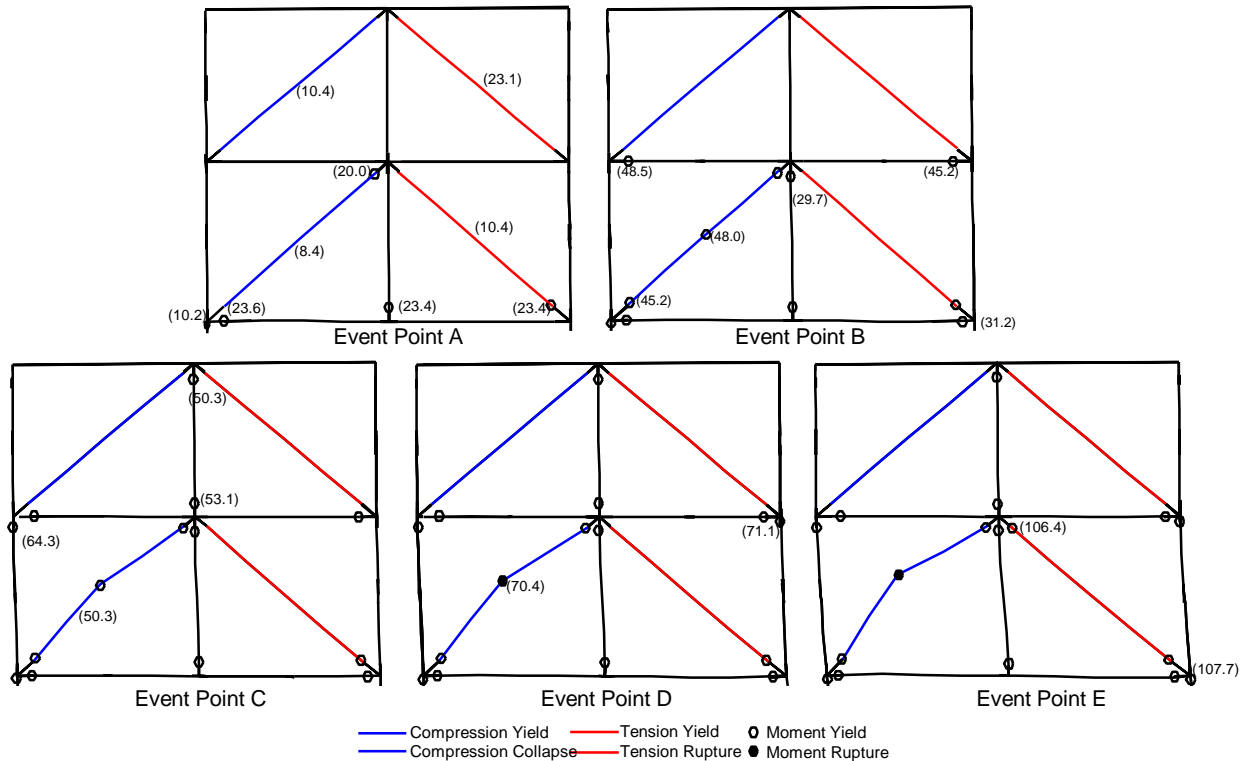


Figure 7 – Prototype Retrofit Tower 3 - Collapse Scenario

The formation of the hinges along the lower compression chevron led directly to the collapse of this member and a subsequent drop in frame load capacity at Event Point C. The prototype pushover analysis was carried to Event Point E at 152 centimeters of displacement although Event Point B was identified as the displacement capacity of the tower. However, after this point, the frame was still carrying well over 65% of the peak frame load capacity and showed no sign of collapse due to superstructure vertical mass.

Longitudinal Pushover - Final Retrofit Tower 3

Following pushover analysis for the prototype retrofit designs for Towers 3, the prototype retrofits were implemented in a global non-linear analysis model and a multi-support base excitation was applied to simulate the design earthquake ground motions. Upon examination of the time history analysis results, it became apparent there still existed deficiencies in the tower's longitudinal displacement capacity. Specifically, the compression legs of Tower 3 had insufficient capacity to prevent its collapse. Also, buckling of the compression chevron braces, which had been predicted in the prototype longitudinal pushover analysis, limited the displacement capacity of the tower and led to collapse of the bridge during the analysis. To remedy this problem, the longitudinal chevrons Tower 3 were braced at their midpoints in order to prevent early buckling.

In addition, the tower legs were pinned at the tops to help reduce the moment demands transferred to the tower legs from the superstructure. Also, to meet the compression demand on the tower legs, the areas of the legs were increased. Finally, large, stout beams were detailed at the bases of the tower legs with post-tensioned hold-downs to restrain the tower legs against uplift and provide for partial moment restraint.

Because the tower legs were partially restrained against rotation, two pushover analyses were conducted with two different boundary conditions at the bases of Tower 3 legs. One analysis evaluated pinned-base tower legs, and the other evaluated fixed-base tower legs, thus bounding the longitudinal displacement capacity of the final Tower 3 retrofit design. The load-deflection curve for the pinned-base tower leg conditions is shown in Figure 8.

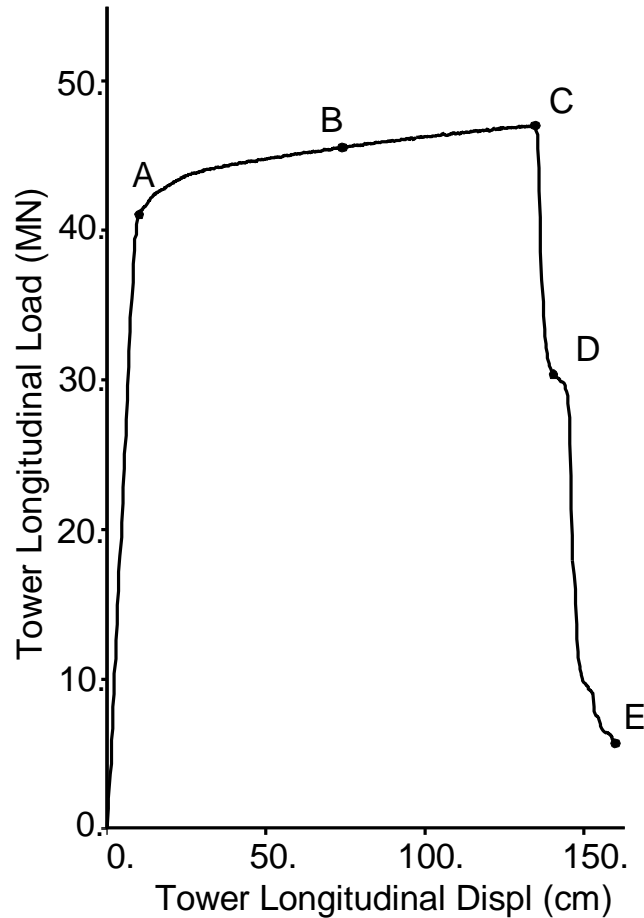


Figure 8 - Final Retrofit Tower 3 - Load-Displacement Curve

At approximately 10 centimeters of tower deflection, Event Point A, the lower compression and tension chevron braces yielded. The stiffness of the frame was reduced as hinges formed and compression and tension yielding continued in the upper chevron members. The maximum load of 47 MN and longitudinal displacement capacity of 139 centimeters occur at Event Point C. Unlike the prototype retrofit, the integrity of the compression chevrons was maintained to a much larger displacement capacity. The implementation of bracing for the chevron members shortened the unbraced length of the chevron, and the buckling of the lower compression chevron was delayed to 143 centimeters without any drop in the lateral load capacity. Event Points D and E show the subsequent buckling of the bottom and top compression chevrons, respectively.

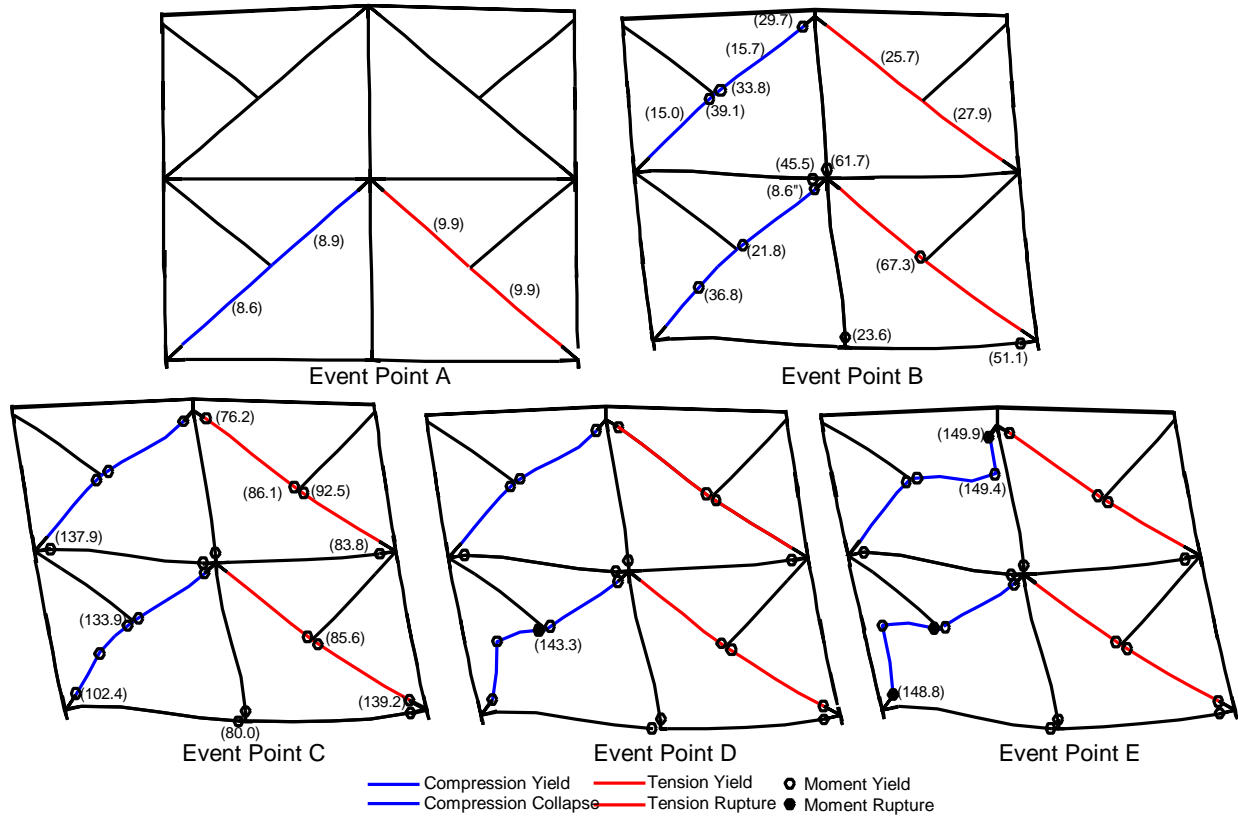


Figure 9 – Final Retrofit Tower 3 - Collapse Scenario

The second longitudinal pushover analysis of the final retrofit design for Tower 3 considered fixed-base tower leg boundary conditions. The differences in pinned-base and fixed-base longitudinal load and displacement capacities for Tower 3 are nominal. The global time history analysis later validated the improvements made to the retrofit design.

DISCUSSION AND CONCLUSIONS

In addition to the overall retrofit goals for the bridge, certain behavioral characteristics of the retrofitted towers were sought, namely:

- Increased ductility of the bridge tower members.
- Provide for Tower 3 to resist all of the longitudinal seismic reactions of the superstructure.
- Significantly increased displacement capacity for the tower without increase in force resistance.

Figure 10 is a comparison of the load-deflection response of the as-built and retrofit Tower 3 structures. Through examination of the changes in tower behavior between as-built and retrofit configurations, the pushover analyses demonstrated that the retrofit measures greatly improved displacement ductility. Most notably, displacement capacity in the longitudinal direction for Tower 3 increased over 650%. Figure 10 substantiates the improvement in the behavior of Tower 3 as-built versus both the prototype retrofit and final retrofit configurations in the longitudinal direction.

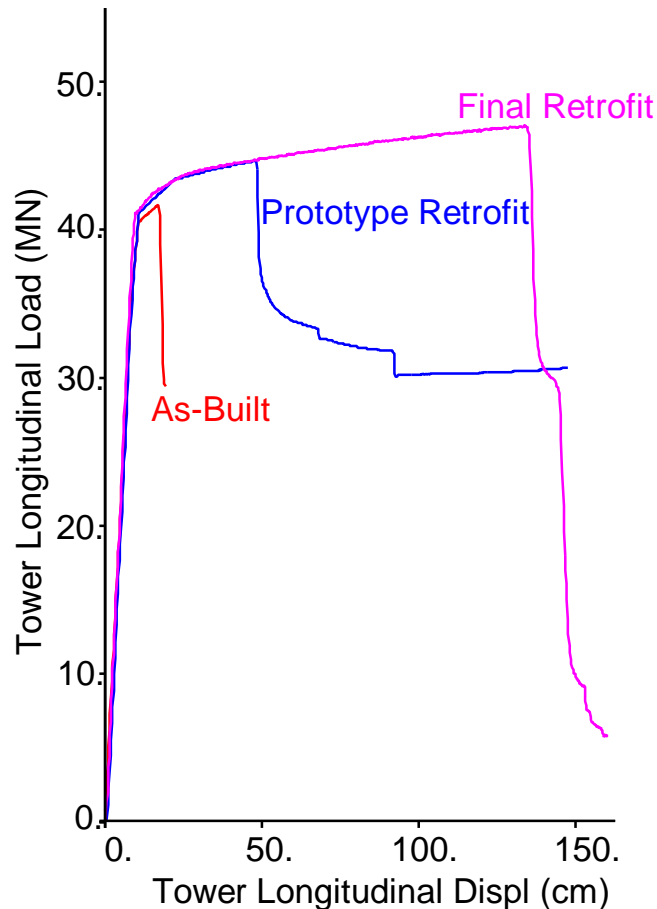


Figure 10 – Comparison of Pushover Results

The improvement in the Tower 3 longitudinal displacement ductility was achieved through a combination of enhancements. Along with strengthening the connections, bracing was added to the chevron elements to prevent buckling. This helped prevent premature hinging of the lower compression chevron and prolonged the buckling collapse mechanism in the lower chevron brace, which resulted in the low displacement capacity of the as-built Tower 3 configuration. Also, the tops of the tower legs were pinned, and stout beams at the base of the tower legs were detailed in conjunction with post-tensioned tie-downs to restrain uplift and rotation at the base of the tower.

In conclusion, this analysis demonstrated the usefulness of non-linear pushover analysis techniques for determining the most efficient retrofit details for steel bridge structures. In addition, the advantages of ADINA's moment-curvature beam element are clearly established.

ACKNOWLEDGEMENTS

This paper was prepared based on the work performed in support of the non-linear analysis activity for the seismic retrofit program of the 1958 Carquinez Strait Bridge. The success of this effort was ensured through the technical input, discussions, reviews, and comments of the non-linear analysis team members: Thomas Ballard, Alexander Krimotat, and Robyn Mutobe, SC Solutions, Inc.; Semyon Treyger, HNTB Corporation; John Hinman, CH2M Hill; Sin-Tsuen Tong and Craig Goings, EQE Engineering & Design; and Abolhassan Astaneh-Asl, University of California at Berkeley. In addition, the support and guidance provided by Steve Thoman, the CH2M Hill Carquinez Bridge retrofit program project manager, and Vong Toan, Caltrans CCMB contract manager, is sincerely appreciated. Also, Frieder Seible, who sat on the Caltrans Peer Review Committee, provided valuable comments and suggestions.

REFERENCES

1. ADINA R&D, Inc., **ADINA-IN Users Manual**, ARD 92-4, Watertown, MA.
2. **1958 Carquinez Strait Bridge Seismic Retrofit Program – Non-Linear Finite Element Analysis**, SC Solutions, Inc., 1997.
3. Astaneh-Asl, Abolhassan, **Inelastic Models of Steel Components of the Carquinez Bridges**, Alamo, CA, 1997.
4. **AASHTO LRFD Bridge Design Specifications**, First Edition, 1994.